Proceedings of the 17th World Congress
The International Federation of Automatic Control
Seoul, Korea, July 6-11, 2008

Image Feature based Navigation of Nonholonomic Mobile Robots with Active Camera

Satoshi Komada* Kousuke Kinoshita**
Tatsuhiko Hirukawa* Junji Hirai******

Department of Electrical and Electronic Engineering, Mie University, Mie, Japan
*(Tel: +059-231-9672; e-mail: komada@elec.mie-u.ac.jp)
* * (Tel: +059-231-9674; e-mail: k-kinoshita@ems.elec.mie-u.ac.jp)
** * (Tel: +059-231-9674; e-mail: hirukawa@ems.elec.mie-u.ac.jp)
****(Tel: +059-231-9671; e-mail: hirai@elec.mie-u.ac.jp)

Abstract: This paper proposes an image feature based navigation method for active camera mounted mobile robots that are affected by nonholonomic constraint. Visual servo is applied to tracking control of the active camera to track targets in the center of image plane. Moreover, posture of nonholonomic mobile robots from targets is controlled by image features of targets that are related to relative distance and angle between robots and targets. It is confirmed that the proposed method can navigate a mobile robot in front of a target with a proper orientation through simulations and experiments.

1. INTRODUCTION

Recently, robots are expected to perform tasks not only in manufacturing fields, such as factories but also in human environment such as hospitals and offices. However, they are dynamical environments that are not prepared for robots like factories. Therefore, robots are required to take surrounding environmental information through external sensors, and to act autonomously based on the information.

Some examples of external sensors for robots are distance sensors using laser or sonar (Nakamoto et al., 2006; Yata et al., 1999) and force sensors. Compared to these sensors, vision sensors such as CCD cameras are very useful for obtaining surrounding environmental information because they can obtain much environmental information visually.

As researches of mobile robots with cameras, a method to control mobile robots by instructed image or landmarks (Makino et al., 2004; Fuchikawa et al., 2006) and an obstacle avoidance method utilizing a potential field formed by camera that placed on ceiling (Katsura et al., 2001) have been proposed.

On the other hand, visual servo methods for nonholonomic mobile robots (Hashimto et al., 2000; Okamoto et al., 2006; Zhang et al., 2002) have been proposed. Visual servo feeds back images obtained from cameras to control robots (Hutchinson et al., 1996). Since the visual servo is "look and move" dynamical visual feedback, where vision sensors are inside feedback loop, robots can act reflexively using visual information. However, visual servo used for usual manipulators can't be applied to wheel type nonholonomic mobile robots as it is. Moreover, motion of mobile robots is restricted extremely because cameras mounted on mobile robots are fixed to execute each method.

This paper proposes an image feature based navigation method in front of targets with proper orientation, where the method expands movable range of nonholonomic mobile robots by applying active cameras for pan angle (Hirukawa et al., 2007). Concretely, visual servo is applied to pan angle of cameras to track targets. Posture of nonholonomic mobile robots from targets is controlled by image features of targets captured by the active cameras that are related to relative distance and angle between robots and targets. Simulation and experimental results show performance of the proposed method.

2. PRECONDITIONS

2.1 Coordinate Systems of Mobile Robot

Fig. 1 shows each coordinate system and a target. The origin of the robot coordinate system R is located in the center of the wheels and the running plane. v and $\dot{\theta}$ are translational velocity toward R_y direction and angular velocity around R_z, respectively. y axis and z axis of the camera coordinate system C coincide with the optical axis and the rotation axis of the active camera, respectively. Δx and Δy are distance of origin for x and y direction from the robot coordinate system to the camera coordinate system, respectively. Moreover, the posture of the mobile robot from the active camera φ is angle deviation from the camera coordinate system C to the robot coordinate system R around z axis. Here, anti-clockwise angles have positive sine.

2.2 Target and Image Plane

In this paper, it is assumed that both mobile robots and targets are placed on the same flat plane as shown in Fig. 1.

Therefore, the distance to targets can be distinguished by vertical position of targets in image plane. Other features such as size of targets, a stereo camera, and so on can be utilized as distance information. The coordinate system of the image plane is determined as shown in Fig. 1, where an optical center of camera coincides with the center of the image plane. In addition, the optical axis is parallel to ground, and the image plane is parallel to the camera coordinate system. It is assumed that the left and right image points $L(x_L, z_L)$ and $R(x_R, z_R)$ toward the target, respectively, can be extracted from the image plane by an appropriate image processing.

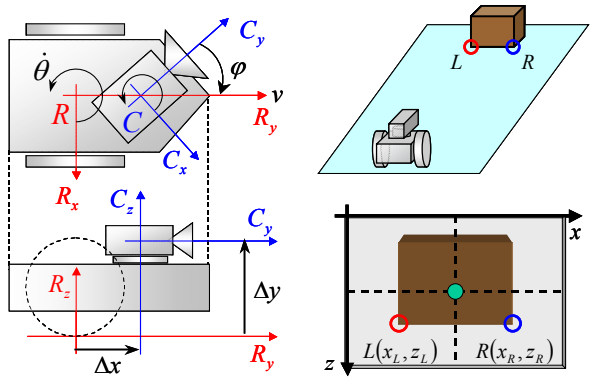

Fig. 1. Coordinate Systems and Target

2.3 Kinematics of Mobile Robots

Velocity to R_y and angular velocity around R_z of the mobile robot v and $\dot{\theta}$ are obtained from angular velocity of wheels $\omega_{R/L}$ as follows.

$$\begin{bmatrix} v \\ \dot{\theta} \end{bmatrix} = \begin{bmatrix} \frac{R_R}{2} & \frac{R_L}{2} \\ \frac{R_R}{T} & -\frac{R_L}{T} \end{bmatrix} \begin{bmatrix} \omega_R \\ \omega_L \end{bmatrix} \quad (1)$$

where $R_{R/L}$ and T are radius of right/left wheels and tread, respectively.

By the inverse matrix of (1), the velocity command and the angular velocity command of the mobile robot v^{ref} and $\dot{\theta}^{ref}$ are transformed to the angular velocity commands of the wheels $\omega_{R/L}^{ref}$ as follows.

$$\begin{bmatrix} \omega_R^{ref} \\ \omega_L^{ref} \end{bmatrix} = \begin{bmatrix} \frac{1}{R_R} & \frac{T}{2R_R} \\ \frac{1}{R_L} & -\frac{T}{2R_L} \end{bmatrix} \begin{bmatrix} v^{ref} \\ \dot{\theta}^{ref} \end{bmatrix} \quad (2)$$

A controller to follow the commands is prepared.

3. PROPOSED NAVIGATION SYSTEM

3.1 Outline

Fig. 2 shows the block diagram of the proposed navigation system for nonholonomic mobile robots with active cameras. Here, ${}^I\mathbf{o}$, $\Delta {}^I\hat{\mathbf{o}}$, and ${}^I\hat{\mathbf{o}}$ show image points of targets obtained from image data, estimated displacement of targets during image processing time, and estimated image points of targets, respectively. Here, the estimated image points ${}^I\hat{\mathbf{o}}$ (Higashi et al., 1998; Komada et al., 2003) are used for control of robots.

The system consists of two parts, i.e. the active camera with visual servo and the controller for navigation of mobile robots. In the both control system image features are utilized to navigate mobile robots in front of targets with a proper orientation.

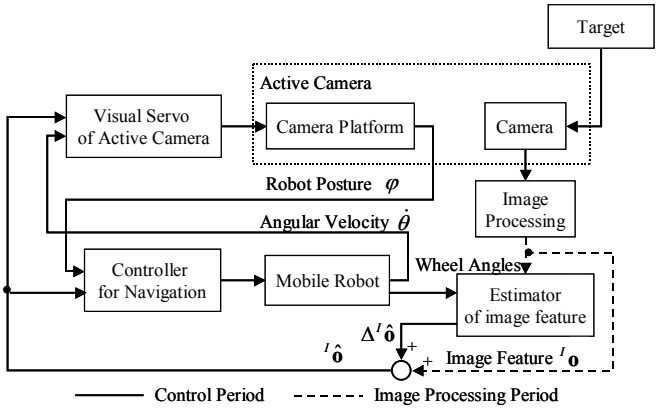

Fig. 2. Proposed Navigation System

3.2 Control of Active Camera

The block "Visual Servo of Active Camera" in Fig. 2 makes the active camera keep the target at the center of image plane while the robot is moving as shown in Fig. 3. Here, feature based visual servo is used for the tracking control of pan angle of the active camera. The angular velocity command of the active camera from the mobile robot $-\dot{\varphi}^{ref}$ is given so that x coordinate of the middle between image points of targets x_m coincides with the center coordinates of image plane x_d as follows:

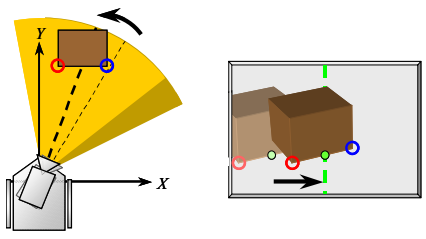

Fig. 3. Visual Servo of Active Camera

$$-\dot{\varphi}^{ref} = J^{-1} \cdot K \cdot (x_d - x_m) - \dot{\theta}$$
$$x_m = \frac{1}{2}(x_L + x_R) \tag{3}$$

where K and $\mathbf{J}$ are a controller gain and an image jacobian matrix from angular velocity of the active camera with respect to the mobile robot to velocity of x coordinates on image plane, respectively. The angular velocity of the mobile robot $\dot{\theta}$ is added as a feed forward term so that the rotational motion of mobile robots doesn't affect the rotational motion of active cameras. The sine of (4) is inverted because the definition of φ is relative angle of mobile robots from active cameras as shown in section *2.1*.

3.3 Control of Mobile Robots

The block "Controller for Navigation" shown in Fig. 2 navigates mobile robots in front of targets with a proper orientation.

3.3.1 Translational Velocity Command

The velocity command v^{ref} in (2) is generated based on distance from robots to targets that is distinguished directly from the image features based on the precondition described in section *2.2*. Fig. 4 shows the graph of the velocity command v^{ref} that is constant until z_R or z_L is more than the threshold value $z_{threshold}$. In order to stop mobile robots in front of targets, the velocity command is decreased by the linear function until z_R or z_L reaches the bottom value of image plane z_{bottom}.

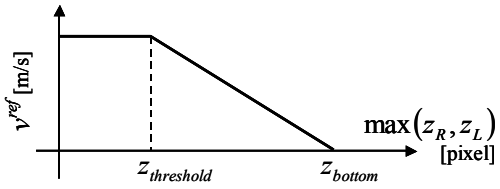

Fig. 4. Velocity Command

3.3.2 Posture Control of Mobile Robots

Posture of mobile robots for targets during movement is controlled to navigate in front of targets with a proper orientation. Since the active camera on the mobile robot is controlled to track targets, the posture of mobile robots from active cameras φ is used. The angular velocity command of mobile robots $\dot{\theta}^{ref}$ in (2) is generated by

$$\dot{\theta}^{ref} = K'(\varphi_d - \varphi) \tag{4}$$

where K' and φ_d are a controller gain and a posture command of mobile robots from active cameras, respectively.

3.3.3 Posture Command from Image Features

Posture command φ_d in (4) is derived from image features of targets obtained from active cameras. Posture of mobile robots for targets can be distinguished by the slope between image points of targets q.

$$q = \frac{z_R - z_L}{x_R - x_L} \tag{5}$$

If robots are in the left, in the right, and in the middle area of targets, the slope q becomes negative, positive, and null, respectively, as shown in Fig. 5.

In order to navigate mobile robots in front of targets with a proper orientation, both the slope between image points of targets q and the posture of mobile robots from active cameras φ must become null simultaneously. In order to realize the situation, q is made null initially and φ is made null secondly as shown in Fig.5. If the slope q is negative and positive, the posture command of mobile robots from active cameras φ_d is $-\pi/2$ and $\pi/2$ so that the slope q decreases as shown in Fig. 5 (a) and (b), respectively. If the slope q is close to zero, the posture command of mobile robots from active cameras φ_d is null so that mobile robots face targets as shown in Fig. 5 (c), i.e. φ becomes null. The strategy can be summarized as follows:

$$\begin{aligned} q < 0 \quad &\cdots \quad \varphi_d = -\frac{\pi}{2} \\ q > 0 \quad &\cdots \quad \varphi_d = \frac{\pi}{2} \\ q = 0 \quad &\cdots \quad \varphi_d = 0 \end{aligned} \tag{6}$$

To avoid chattering of mobile robots, a smooth function of the slope q is adopted as shown in Fig. 6 and (7).

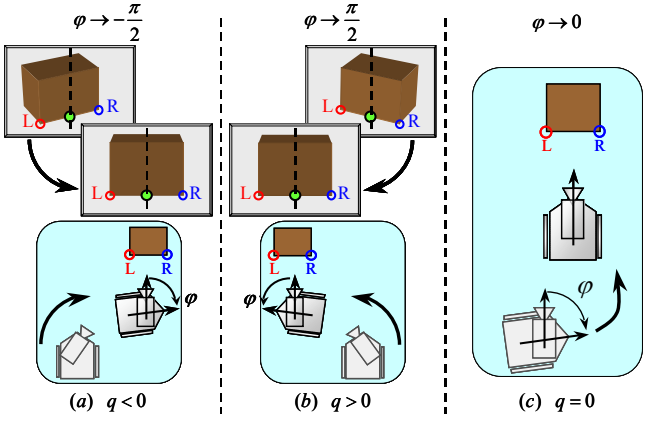

Fig. 5. Posture Command φ_d

$$\varphi_d = \begin{cases} -\frac{\pi}{2} + \frac{\frac{\pi}{2}}{1+\exp(-600\cdot q - 27)} & \cdots q < 0 \\ 0 & \cdots q = 0 \\ \frac{\frac{\pi}{2}}{1+\exp(-600\cdot q + 27)} & \cdots q > 0 \end{cases} \quad (7)$$

Here, the parameters are adjusted through repetition of navigation.

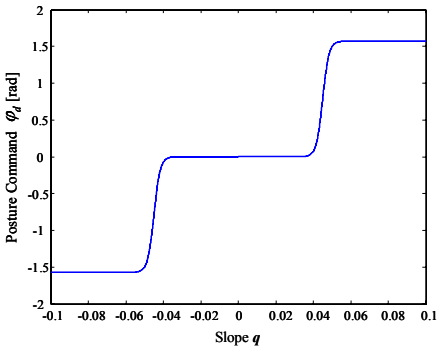

Fig. 6. Posture Command Function φ_d

3.3.4 Posture Command with Distance Consideration

The posture command of mobile robots from active cameras φ_d shown in Fig. 6 and (7) make mobile robots to adjust their position in front of targets initially. Therefore, their trajectory becomes long if the distance from mobile robots to targets is long. In order to prevent the phenomenon, reduction of the slope q shown in Fig. 5 (a) and (b) is inhibited if the distance is long. Fig. 7 and (8) show the weight for the posture command of mobile robots from active cameras.

$$W = \frac{1}{1+\exp(-0.14\cdot z_m + 39.2)} \quad (8)$$

$$z_m = \frac{1}{2}(z_L + z_R)$$

where z_m is the vertical position of the middle between image points of targets that is related to distance to targets. The weight becomes small if z_m is close to the vanishing line 240[pixel] as shown in Fig. 7, which means that the target exist far from the robot.

The weight shown in (8) is multiplied to the posture command of mobile robots from active cameras φ_d shown in Fig. 6 and (7) to obtain a new command φ_d^{new} shown in Fig. 8.

$$\varphi_d^{new} = W \cdot \varphi_d \quad (9)$$

Therefore, the mobile robots go straight to targets if the distance is long by using the posture command of mobile robots from active cameras φ_d^{new} shown in Fig. 8 and (9). The parameter of the weight is also determined through repetition of navigation.

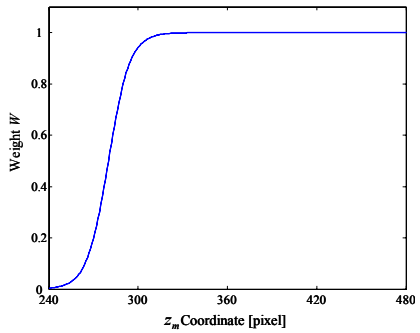

Fig. 7. Weight Function W

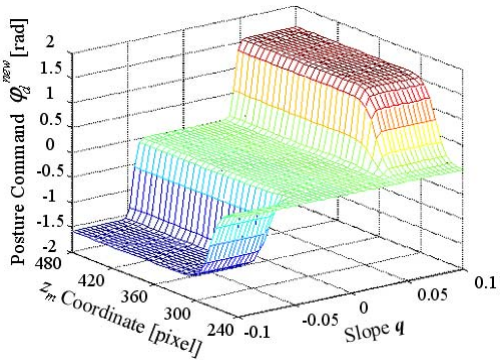

Fig. 8. Posture Command Function φ_d^{new}

4. RESULTS

4.1 Simulation Conditions

To confirm the effectiveness of the proposed method, simulation is performed by an active camera mounted nonholonomic mobile robot as shown in Fig. 1. Table 1 and Table 2 show parameters of the camera and control, respectively.

Table 1 Parameters of camera

Focal length	[m]	0.008
Number of pixel to x direction	[pixel/m]	640/0.0054
Number of pixel to z direction	[pixel/m]	480/0.0047
Δx	[m]	0.17
Δy	[m]	0.2

Table 2 Parameters of control

Control Period	[ms]	1
Image Processing Period	[ms]	50
Controller Gain of Active Camera K		15
Controller Gain of Mobile Robot K'		1
v^{ref}	[m/s]	0.4
$z_{threshold}$	[pixel]	320
z_{bottom}	[pixel]	480

4.2 Simulation Results

Fig. 9 shows simulation results using the posture commands φ_d shown in (7) and Fig. 6 and φ_d^{new} shown in (9) and Fig. 8. The result is plotted on the world coordinate fixed to an initial pose of the mobile robot. It is understood that the mobile robot is navigated in front of the targets by these methods with a proper orientation. The trajectory of φ_d^{new} is shorter than the one of φ_d because of the weight for distance as shown in Fig. 7 and (8). Table 3 shows the final posture of the mobile robot from the active camera φ, final posture of the mobile robot θ with respect to the world coordinate from X-axis, and movement time of the result shown in Fig.9. Even though the final poses are almost the same, the trajectory and movement time becomes small by the posture command weighted by distance φ_d^{new}.

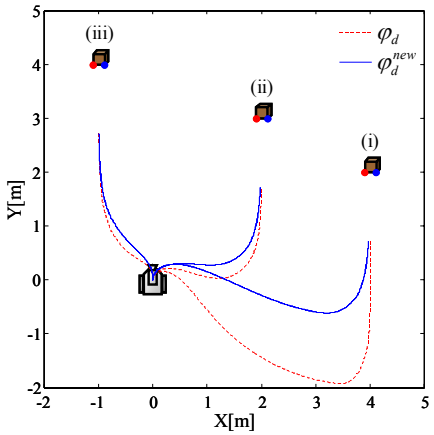

Fig. 9. Simulation Results by φ_d and φ_d^{new}

Table 3. Final Postures and Movement Time

φ_d / φ_d^{new}	(i)	(ii)	(iii)
θ[deg]	90.0 88.0	89.5 88.3	90.2 90.3
φ[deg]	0.00 -1.09	-0.22 -0.86	0.04 0.16
Time[s]	19.4 14.2	10.0 9.3	9.1 9.0

4.3 Experimental Conditions

The image processing period is 33[ms]. Other parameters are the same as the simulation parameters shown in Table 1 and Table 2. Moreover, image feature estimation shown in Fig. 2 is not performed in experiment. Here, only φ_d^{new} is tested.

The experimental environment is simplified in order to make image feature extraction easy. Two white marks at intervals of 0.2[m] are placed on the running plane as a target. Other 3×3[m] running plane and wall are made black.

4.4 Experimental Results

Navigation in front of the target is tested experimentally. Here, the camera on the mobile robot catches the middle point of the image feature points of the target in the vicinity of the center of the image plane in the initial state.

Fig. 10 shows running trajectories of each initial condition. Table 4 shows each posture of the mobile robot in absolute coordinate system θ and each posture of the mobile robot from the active camera φ at arrival. Here, the trajectory in Fig. 10 is obtained from a dead reckoning method which is not utilized in the proposed method. The experimental results show trajectories without long detours and the accuracy of the arrival posture as well as the simulation results.

Fig. 11 and Fig.12 are results of (i) in Fig. 10. Fig. 11 shows that the active camera tracks the target in the middle of the image plane. Fig. 12 shows the detected image features and the derived posture command of the mobile robot φ_d^{new}.

The effectiveness of the proposed method is confirmed from the above results.

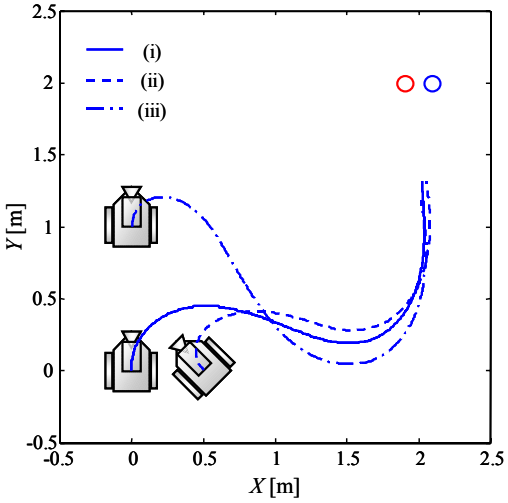

Fig. 10. Trajectories

Table 4. Final Postures

Condition	θ[deg]	φ[deg]
(i)	89.103	-1.605
(ii)	91.285	-1.243
(iii)	92.411	-1.297

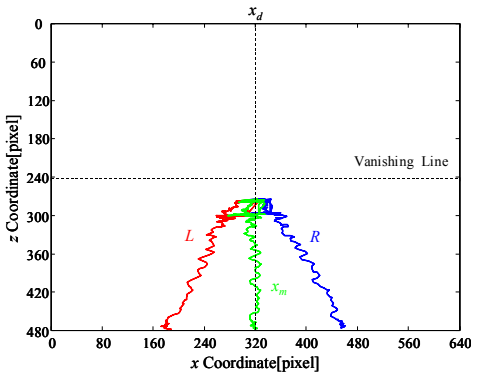

Fig. 11. Target on Image Plane

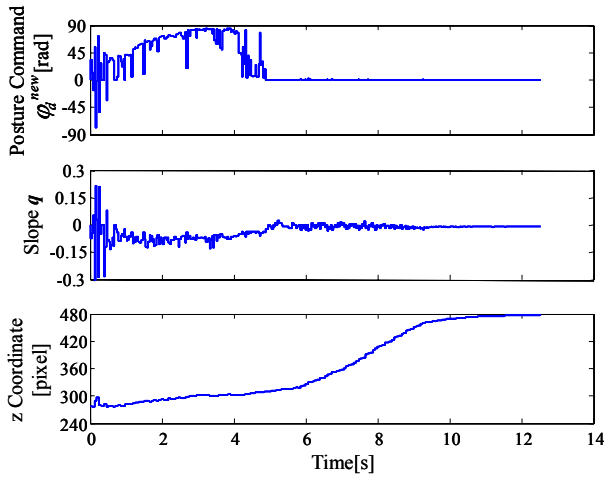

Fig. 12. Time response of Posture Command φ_d^{new}

5. CONCLUSIONS

This paper proposes a navigation method of nonhoronomic mobile robots with active cameras. Visual servo is applied to pan angle of active cameras during control of nonhoronomic mobile robots to keep targets in image. Since slope of targets q and the vertical position of targets z_m in image plane are related to relative angle and distance from mobile robots to targets, respectively, these image features are utilized to navigate mobile robots in front of targets. Here, control of the mobile robot is performed based on the posture of the mobile robot from the active camera using the visual servo. Moreover, the simulation and experimental results show that the proposed method enables navigation of the nonholonomic mobile robot with the active camera to some targets with a proper orientation. On the other hand, it is necessary to design a method under the environment where obstacles exist.

REFERENCES

Y. Fuchikawa, S. Kurogi, K. Matsuo, S. Miyamoto and T. Nishida (2006). Mobile Robot Navigation Using Guideposts and a Single Camera. *The Society of Instrument and Control Engineers*. **Vol.42**, No.1, pp.62-69.

K. Hashimoto, A. So and T. Noritsugu (2000). Visual Feedback Control of Cart based on Path Planning in Image Plane. *Transactions of the Japan Society of Mechanical Engineers. C*, **Vol.66**, No.652, pp.172-178.

S. Higashi, S. Komada, M. Ishida, and T. Hori (1998). Obstacle Avoidance of Redundant Manipulators on Visual Servo System Using Estimated Image Features. In *Proc. International Workshop on Advanced Motion Control*, pp.165–170.

T. Hirukawa, S. Komada, and J. Hirai (2007). Image Feature based Navigation of Nonholonomic Mobile Robots with Active Camera. In Proceedings of SICE Annual Conference 2007 in Takamatsu, pp.2502-2506.

Seth Hutchinson, Gregory D. Hager, and Peter I. Corke (1996). A Tutorial on Visual Servo Control. *IEEE Transactions on Robotics and Automation*, vol. 12, no. 5, pp.651–670.

S. Katsura and K. Ohnishi (2001). Dynamic Obstacle Avoidance of Autonomous Mobile Robot Based on Probabilistic Potential Field. In: *The Transactions of the Institute of Electrical Engineers of Japan. D, A publication of Industry Applications Society*. **Vol.121**, No.12, pp.1284-1290.

S. Komada, M. Yoshida, and T. Hori (2003). Visual Servoing of Robots using Estimated Image Features. *The Transactions of the Institute of Electrical Engineers of Japan. D*, Vol. 123, No. 10, pp. 1200-1205.

H. Makino, S. Yamamoto, T. Azukizawa and T. Hashimoto (2004). An Experiment on Mobile Robot Navigation by Instruction Using Digital Camera Images. *Review of the Faculty of Maritime Sciences, Kobe University*, **Vol.1**, pp.131-136.

T. Nakamoto, A. Yamashita, and T. Kaneko (2006). 3-D Map Generation in a Dynamic Environment by a Mobile Robot Equipped with Laser Range Finders. *IEICE technical report. Welfare Information technology*, Vol. 106, No. 144, pp. 25-30.

K. Okamoto, K. Yamaguchi and N. Maru (2006). Following Motion Control of the Mobile Robot by Using Linear Visual Servoing. *Transactions of the Japan Society of Mechanical Engineers. C*, **Vol.72**, No.718, pp. 1840-1847.

T. Yata, A. Ohya, and S. Yuta (1999). A Fast and Accurate Reflecting Points Measurable Sonarring System. *Journal of the Robotics Society of Japan*, Vol. 17, No. 8, pp. 1173-1182.

H. Zhang, and J. P. Ostrowski (2002). Visual Motion Planning for Mobile Robots. *IEEE TRANSACTION ON ROBOTICS AND AUTOMATION*, **Vol.18**, No.2, pp.199-208.